Frequency Estimation in Multipath Rayleigh-Sparse-Fading Channels

Yuriy V. Zakharov, *Member, IEEE*, Vladimir M. Baronkin, and Tim. C. Tozer, *Member, IEEE*

***Abstract*—Maximum-likelihood (ML) data-aided frequency estimation in multipath Rayleigh-fading channels with sparse impulse responses is investigated. We solve this problem under the assumption that the autocorrelation matrix of the pilot signal can be approximated by a diagonal matrix, the fading of different path amplitudes are independent from each other, and the additive noise is white and Gaussian. The ML frequency estimator is shown to be based on combining nonlinearly transformed path periodograms. We have derived the nonlinear function for the two cases: known and unknown fading variances. The new frequency estimators lead, in particular cases, to known ML frequency estimators for nonsparse multipath fading channels. The use of *a priori* information about the mean number of paths in the channel allows a significant improvement of the accuracy performance. Exploiting the sparseness of the channel impulse response is shown to significantly reduce the threshold signal-to-noise ratio at which the frequency error departs from the Cramer–Rao lower bound. However, precise knowledge of the channel sparseness is not required in order to realize this improvement.**

***Index Terms*—Fading channels, frequency estimation, maximum likelihood (ML) estimation, multipath channels, Rayleigh channels.**

I. Introduction

In MANY communication scenarios, a receiver has to perform both frequency and timing synchronization in a large frequency and timing uncertainty. The synchronization problem becomes especially difficult if the propagation channel is multipath and fading. In mobile channels, multipath components experience different Doppler offsets; however, if the mobile speed and the carrier frequency are relatively low, the frequency offset is mainly due to the difference between carriers of the receiver and transmitter, and the assumption of equal frequency offsets for all multipath components can be accepted. Under such an assumption one approach to solve the synchronization problem is to estimate and compensate for the frequency offset, and then perform the timing synchronization (or equalization). This work is devoted to the first stage: frequency estimation in multipath Rayleigh-fading channels with an unknown sparse impulse response. Specifically, we consider a maximum likelihood (ML) data-aided frequency estimation [1].

Manuscript received November 4, 2002; revised May 1, 2003; accepted June 17, 2003. The editor reviewing this paper and approving it for publication is J. Cavers. The material in this paper was presented in part at the IEEE International Conference on Communication, New York, April 2002.

Y. V. Zakharov and T. C. Tozer are with the Communication Research Group, Department of Electronics, University of York, York YO10 5DD, U.K. (e-mail: yz1@ohm.york.ac.uk; tct@ohm.york.ac.uk).

V. M. Baronkin is with the N. N. Andreev Acoustics Institute, 117036 Moscow, Russia (e-mail: vbar@online.ru).

Digital Object Identifier 10.1109/TWC.2004.833465

In burst data transmission, a pilot signal is used for synchronization, and this should be as short as possible in order not to decrease the spectral efficiency of the communication system. This requires a high accuracy performance of the channel estimator. The performance should be high enough to accurately compensate for the channel distortion. This can be achieved by using the most efficient estimators, which are known to be ML estimators. The structure and performance of the ML estimator depends on the channel and signal model; the more *a priori* information that can be introduced into the model, the higher the performance that can be achieved. Knowledge of the sparseness of the channel impulse response is information which, when introduced in a channel model, can lead to more advanced estimators. We use the term "sparseness" to emphasise that the number of multipath components is much fewer than the number of resolved delays within the timing uncertainty interval.

An ML frequency estimator for multipath Rayleigh-fading channels, i.e., when the path amplitudes are complex Gaussian random variables, has been presented in [2]. For channels with independent fading and unknown variances of path amplitudes the ML frequency estimator combines nonlinearly transformed path periodograms for all possible delays, and a maximum of the combined periodogram over a frequency acquisition range Ω indicates the frequency estimate. The scheme of the estimator is shown in Fig. 1. For each possible delay τ_m, $m = 1, \ldots, M$, a path periodogram $|F_{\omega,m}|^2$ ($\omega \in \Omega$) is calculated. It is defined as a squared module of a discrete Fourier transform (DFT) of the product of the received signal $z(t)$ and the delayed conjugate transmitted signal $s^*(t - \tau_m)$. The path periodogram is normalized by a factor $\xi_m = (\sigma^2 \gamma_{mm})^{-1}$, which depends on the noise variance σ^2 and the autocorrelation γ_{mm} of the transmitted (pilot) signal $s(t)$, and a nonlinear transform $g(\cdot)$ of the normalized path periodogram is performed. The results of the nonlinear transforms are combined in a statistic whose maximum indicates the frequency estimate. The nonlinear function $g(x)$ is defined as [2]

$$g(x) = g_1(x) = \begin{cases} 0, & \text{if } 0 \le x < 1 \\ x - \ln(x) - 1, & \text{if } x \ge 1. \end{cases} \quad (1)$$

The nonlinear function $g(x)$ allows the frequency estimator to accumulate the periodograms of strong paths rejecting weak paths.

An ML frequency estimator for multipath deterministic channels has been derived in [3] and [4]. We use the term "deterministic" to emphasise that path amplitudes are unknown deterministic parameters. In [5], an ML frequency estimator

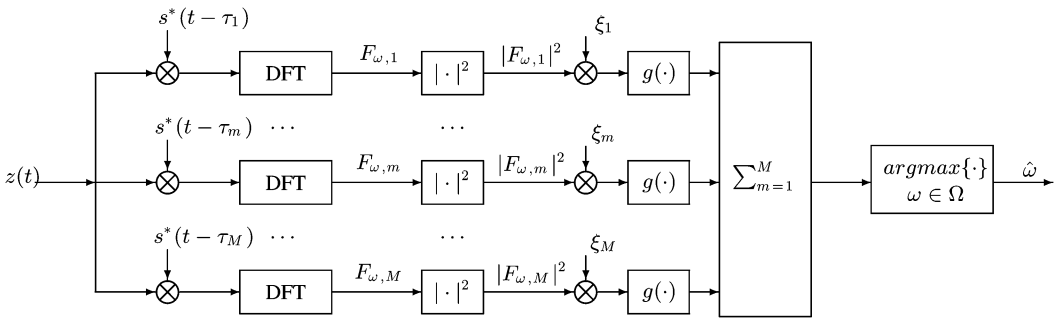

Fig. 1. Frequency estimator with nonlinear transformation of path periodograms.

for multipath deterministic channels with a sparse impulse response has been presented. It is interesting that for such sparse channels, the frequency estimator has the same structure as that depicted in Fig. 1; the only difference is in the nonlinear transform. Now

$$g(x) = g_2(x) = \ln(pe^x + 1 - p) \tag{2}$$

where p is a probability of appearance of a path with a nonzero amplitude at delay τ_m. The case $p = 1$ means that all the path amplitudes are not zero. For $p = 1$, we have $g_2(x) = x$ leading to a linear weight addition of the path periodograms; such an estimator coincides with the ML frequency estimator for multipath channels with unknown deterministic path amplitudes [4]. The behavior of the function $g_2(x)$ for small x significantly affects frequency errors at low signal-to-noise ratios (SNRs) and defines the SNR threshold at which the frequency error departs from the Cramer–Rao lower bound (CRLB). The nonlinear transform reduces the SNR threshold with respect to that of the frequency estimator with a linear weight addition of the path periodograms; the ability of a frequency estimator to operate at low SNRs is very important for many practical applications.

The purpose of this paper is to derive an ML frequency estimator for multipath Rayleigh-fading channels with sparse impulse responses. We will show that this frequency estimation may also be realized by the scheme depicted in Fig. 1, but with new nonlinear transforms. The nonlinear transform differs for the two cases: known and unknown fading statistics. We will also show that the new proposed frequency estimators generalize ML frequency estimation in multipath fading channels because previously known estimators are shown to be particular variants of the frequency estimators proposed in this paper. We will present simulation results and compare the estimation accuracy for the different nonlinear transforms of path periodograms.

This paper is organized as follows. Section II describes channel and signal models. In Section III, we derive the ML frequency estimator for multipath Rayleigh-sparse-fading channels. In Section IV, we present simulation results, and Section V contains conclusions.

II. Signal Model

Using complex-envelope notation, the observed signal can be modeled as

$$z(iT) = A(iT)e^{j\omega iT} + n(iT), \qquad i = 0, \ldots, N-1 \tag{3}$$

where T is the sampling interval, ω an unknown frequency offset to be estimated, and N the number of samples observed. The additive complex white Gaussian noise samples $n(iT)$ have variance σ^2. The complex envelope $A(iT)$ can be represented as

$$A(iT) = \sum_{m=1}^{M} \chi_m a_m s(iT - \tau_m) \tag{4}$$

where $s(iT)$ is the transmitted (pilot) signal, $\{a_m\}_{m=1}^{M}$ are unknown complex path amplitudes, $\{\tau_m\}_{m=1}^{M}$ are delays of the paths, and $\{\chi_m\}_{m=1}^{M}$ are independent binary random variables: $\chi_m \in \{0, 1\}$. We consider $\{\tau_m\}_{m=1}^{M}$ as an admissible set of delays, for example, $\tau_m = (m-1)T$. The model (3) is based on the assumption that all paths have the same frequency offset; this is valid, for example, when there exists a frequency offset between carrier frequencies of the transmitter and the receiver, and the frequency offsets due to the Doppler effect are negligible. We assume that the appearance of a path with a nonzero amplitude at delay τ_m is a random event with probability $p(\chi_m = 1) = p_0$ and is independent of appearances of paths with nonzero amplitudes at the other delays. The number of paths L with nonzero amplitudes within the delay uncertainty range $[\tau_1, \ldots, \tau_M]$ is a random value with mean $E\{L\} = Mp_0$, where $E\{\cdot\}$ denotes the statistical expectation; for example, if $M = 120$ and $p_0 = 0.02$, we have the mean number of significant paths $E\{L\} = 2.4$. We also assume that the pilot signal possesses a diagonal correlation matrix with elements

$$\begin{aligned}\gamma_{mn} &= \sum_{i=0}^{N-1} s^*(iT - \tau_m)s(iT - \tau_n) \\ &= \delta_{mn} \sum_{i=0}^{N-1} |s(iT - \tau_m)|^2 \end{aligned} \tag{5}$$

where δ_{mn} is the Dirac delta function and $(\cdot)^*$ denotes complex conjugate. Note that (5) can be only approximately true, for example, for long pseudonoise sequences. We will show below that this approximation affects the frequency estimates at only high SNRs.

The signal model (3) can be arranged in matrix form as

$$\mathbf{z} = \mathbf{\Lambda}_\omega \mathbf{\Phi} \mathbf{X} \mathbf{a} + \mathbf{n} \tag{6}$$

where $\mathbf{z}$ and $\mathbf{n}$ are $N \times 1$ vectors with elements $z(iT)$ and $n(iT)$, respectively; $\mathbf{a}$ is an $M \times 1$ vector of complex path amplitudes: $\mathbf{a} = [a_1, \ldots, a_M]^T$; $\mathbf{X} = \text{diag}[\mathbf{x}]$ is a diagonal $M \times M$ matrix; $\mathbf{x} = [\chi_1, \ldots, \chi_M]^T$ is an $M \times 1$ vector of independent random

binary variables: $\chi_m = 1$ with the probability p_0, $\chi_m = 0$ with the probability $(1 - p_0)$; $\mathbf{\Phi}$ is an $N \times M$ matrix with elements $[\mathbf{\Phi}]_{im} = s(iT - \tau_m)$; and $\mathbf{\Lambda}_\omega = \text{diag}[1, e^{j\omega T}, \ldots, e^{j\omega(N-1)T}]$. Here, $[\cdot]^T$ denotes matrix transposition.

The probability density function (pdf) of the received signal vector $\mathbf{z}$ (subject to fixed ω, $\mathbf{x}$, and $\mathbf{a}$) can be written as

$$\mathbf{p}(\mathbf{z}|\omega, \mathbf{x}, \mathbf{a}) = \frac{1}{\pi^N |\mathbf{R_n}|} \times \exp\left\{-(\mathbf{z} - \mathbf{\Lambda}_\omega \mathbf{\Phi X a})^H \mathbf{R_n}^{-1} (\mathbf{z} - \mathbf{\Lambda}_\omega \mathbf{\Phi X a})\right\} \quad (7)$$

where $(\cdot)^H$ denotes Hermitian transposition, $|\mathbf{R_n}|$ denotes the determinant of the matrix $\mathbf{R_n}$, and $\mathbf{R_n} = E\{\mathbf{n}\mathbf{n}^H\}$ is the noise covariance matrix. The noise samples are assumed to be uncorrelated, i.e., $\mathbf{R_n} = \sigma^2 \mathbf{I}_N$ where $\mathbf{I}_N$ is an $N \times N$ identity matrix.

We consider Rayleigh-fading channels, i.e., the path amplitudes $\{a_m\}_{m=1}^M$ are complex-valued zero-mean random variables with the Gaussian pdf

$$\mathbf{f_a}(\mathbf{a}) = \frac{1}{\pi^M |\mathbf{R_a}|} \exp\left\{-\mathbf{a}^H \mathbf{R_a}^{-1} \mathbf{a}\right\} \quad (8)$$

where $\mathbf{R_a} = E\{\mathbf{a}\mathbf{a}^H\}$ is the fading covariance matrix. The complex path amplitudes are assumed to be uncorrelated, i.e., the fading covariance matrix is

$$\mathbf{R_a} = E\{\mathbf{a}\mathbf{a}^H\} = \text{diag}\left(\sigma_1^2, \sigma_2^2, \ldots, \sigma_M^2\right) \quad (9)$$

where σ_m^2 is the variance of the path amplitude a_m.

The pdf of the vector $\mathbf{x}$ can be written as

$$\mathbf{f_x}(\mathbf{x}) = \prod_{m=1}^{M} [p_0 \delta(\chi_m - 1) + (1 - p_0)\delta(\chi_m)] \quad (10)$$

where $\delta(\cdot)$ is the Dirac delta function.

The described channel model possesses the following drawbacks.

1) There is a nonzero probability that the number of paths with nonzero amplitudes is equal to zero, which from (4) results in $A(iT) \equiv 0$. This probability is calculated as $\Pr(0) = (1 - p_0)^M$. If, for example, $p_0 = 0.02$ and $M = 120$ we have a relatively high probability of such an event: $\Pr(0) \approx 0.09$. This situation does not make any physical sense; therefore, in our simulation below, in each simulation trial we repeat generating the delay set $\{\tau_m\}_{m=1}^M$ until the channel has at least one path with a nonzero amplitude (i.e., at least one number χ_m, $m = 1, \ldots, M$, is equal to one).
2) In the signal model (4), the path delays τ_m are taken as integer multiples of the sampling period T, i.e., $\tau_m = (m - 1)T$. This means that τ_m does not represent the delay of a physical multipath component but rather the mth delay of the equivalent tapped-delay-line that models the transmission channel. Then, the complex coefficient a_m represents the sample of the overall channel impulse response taken at instant τ_m. Denoting by $\{t_l\}_{l=1}^L$ and $\{\alpha_l\}_{l=1}^L$ the delays and complex gains of the physical multipath components (L being the effective number of multipath components), the coefficients a_m are given by

$$a_m = \sum_{l=1}^{L} \alpha_l h[(m-1)T - t_l] \quad (11)$$

where $h(t)$ denotes the convolution between the impulse responses of the transmit and receive filters. The path gains $\{\alpha_l\}_{l=1}^L$ can be modeled as independent zero-mean Gaussian random variables. However, denoting $\sigma_l^2 = E\{|\alpha_l|\}$ as the mean power of the lth physical path, from (11), it is seen that

$$E\left\{a_m a_{m-k}^*\right\} = \sum_{l=1}^{L} \sigma_l^2 h[(m-1)T - t_l] \times h^*[(m - 1 - k)T - t_l] \quad (12)$$

i.e., the coefficients a_m cannot be assumed statistically independent as in (9).

However, the ML approach applied to this channel model leads to a frequency estimator possesing improved accuracy performance in more realistic channels. We demonstrate this in the following by simulating our frequency estimation algorithm in a multipath channel with a fixed number of multipath components L and arbitrary fractional delays t_l within a delay uncertainty interval $[0, (M-1)T]$.

III. Algorithm Derivation

In order to derive the ML frequency estimation algorithm we use the Bayesian approach by integrating out the nuisance parameters a_m and χ_m, $m = 1, \ldots, M$. We can write

$$\mathbf{p}(\mathbf{z}|\omega) = \int_{-\infty}^{\infty} \mathbf{p}(\mathbf{z}|\omega, \mathbf{x}, \mathbf{a}) \mathbf{f_a}(\mathbf{a}) \mathbf{f_x}(\mathbf{x}) d\text{Re}[\mathbf{a}] d\text{Im}[\mathbf{a}] d\mathbf{x} \quad (13)$$

where $\text{Re}[\cdot]$ and $\text{Im}[\cdot]$ denote, respectively, the real and imaginary parts of a complex-valued number, the pdf $\mathbf{p}(\mathbf{z}|\omega, \mathbf{x}, \mathbf{a})$ is defined by (7), the pdf $\mathbf{f_a}(\mathbf{a})$ is defined by (8), and the pdf $\mathbf{f_x}(\mathbf{x})$ is defined in (10). The ML frequency estimator is found by maximizing the function $\mathbf{p}(\mathbf{z}|\omega)$

$$\hat{\omega} = \arg\max_{\omega \in \Omega} \{\mathbf{p}(\mathbf{z}|\omega)\} = \arg\max_{\omega \in \Omega} \{\ln[\mathbf{p}(\mathbf{z}|\omega)]\} \quad (14)$$

where Ω is the frequency acquisition range, e.g., $\Omega = [-\pi, \pi]$. From the Appendix, we have

$$\mathbf{p}(\mathbf{z}|\omega) = c_0 \prod_{m=1}^{M} \left[\frac{p_0}{1 + \alpha_m} \exp\left(\frac{G_{\omega,m}\alpha_m}{1 + \alpha_m}\right) + (1 - p_0)\right] \quad (15)$$

where the coefficient c_0 does not depend on the frequency ω, $\alpha_m = \sigma_m^2 \gamma_{mm}/\sigma^2$, $G_{\omega,m} = \xi_m |F_{\omega,m}|^2$, $\xi_m = (\sigma^2 \gamma_{mm})^{-1}$, and $F_{\omega,m}$ are the DFTs of the product $z(iT)s^*(iT - \tau_m)$

$$F_{\omega,m} = \sum_{i=0}^{N-1} z(iT) s^*(iT - \tau_m) e^{-j\omega iT}. \quad (16)$$

After taking the logarithm in (15), it is seen that the ML frequency estimation is based on calculation of path periodograms

$|F_{\omega,m}|^2$, normalization of the periodograms by factors ξ_m, and combining nonlinear transforms, as shown in Fig. 1.

The pdf $\mathbf{p}(\mathbf{z}|\omega)$ in (15) depends on the parameter p_0 which is assumed to be known and the parameters $\{\alpha_m\}_{m=1}^M$ which can be either known or unknown. To emphasize the case of unknown parameters α_m we will use the notation

$$\mathbf{p}(\mathbf{z}|\omega) = \mathbf{p}\left(\mathbf{z}|\omega, \{\alpha_m\}_{m=1}^M\right).$$

In the following, we consider the two cases: 1) the fading variances $\{\sigma_m^2\}_{m=1}^M$ are known, and 2) the fading variances $\{\sigma_m^2\}_{m=1}^M$ are unknown.

A. Known Fading Variances

This case corresponds to the situation when the frequency estimator knows the power delay profile. It is rather an impractical situation; however, it is characterized by an additional knowledge of the channel and should lead to a smaller estimation error than the second case. In some sense, we can consider this as a lower bound of the frequency error for frequency estimation with unknown fading variances considered in Section III-B.

By using (15), we can write the ML frequency estimate (14) as

$$\begin{aligned}\hat{\omega} &= \arg\max_{\omega\in\Omega}\{\ln[\mathbf{p}(\mathbf{z}|\omega)]\} \\ &= \arg\max_{\omega\in\Omega}\left\{\sum_{m=1}^{M} g(G_{\omega,m},\alpha_m)\right\} \end{aligned} \tag{17}$$

where

$$\begin{aligned} g(x,\alpha) &= g_3(x,\alpha) \\ &= \ln\left[\frac{p}{1+\alpha}\exp\left(\frac{x\alpha}{1+\alpha}\right)+(1-p)\right] \end{aligned} \tag{18}$$

and $p = p_0$. Thus, we have found the ML frequency estimator for multipath fading channels with a sparse impulse response when the probability p_0 of appearance of a path with a nonzero amplitude a_m at delay τ_m is known and variances of path amplitudes σ_m^2 (or, the same, the parameters α_m) are also known.

This ML estimator is realized by the scheme in Fig. 1 where $\xi_m = (\sigma^2\gamma_{mm})^{-1}$ and the nonlinear function $g(x,\alpha)$ is defined in (18). This nonlinear function is specific to each path and depends on the SNR α_m of the multipath component. The function $g_3(x,\alpha)$ is depicted in Fig. 2 for different values of the parameters p and α. For a fixed α, as p decreases the range of x where the function $g_3(x,\alpha)$ is close to zero increases, i.e., the smaller the probability of a nonzero path amplitude the higher is the "cutoff" level of the function $g_3(x,\alpha)$. For a fixed p, as α increases the slope of the function $g_3(x,\alpha)$ increases; i.e., the higher the SNR of a multipath signal component, the more the component contributes to the output statistic.

It is interesting to consider a special case of $p_0 = 1$ which means that all the path amplitudes have nonzero variances. In this case, we obtain from (18) that

$$g_3(x,\alpha) = -\ln(1+\alpha) + \frac{x\alpha}{(1+\alpha)} \tag{19}$$

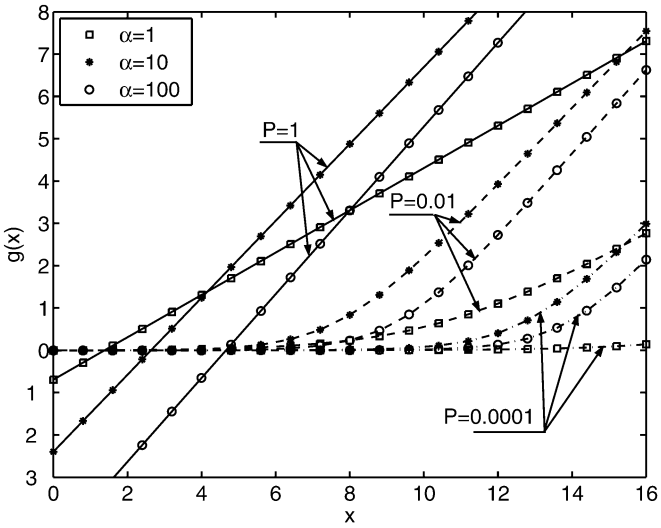

Fig. 2. Nonlinear function $g_3(x,\alpha)$ for different values of the parameters p and α.

i.e., the function $g_3(x,\alpha)$ is now linear. The first addition in $g_3(x,\alpha)$ does not depend on x (i.e., on the frequency ω) and, therefore, it does not affect the frequency estimate $\hat{\omega}$; it can be omitted, and we can rewrite (17) as

$$\hat{\omega} = \arg\max_{\omega\in\Omega}\left\{\sum_{m=1}^{M}\xi_m|F_{\omega,m}|^2\right\} \tag{20}$$

where now

$$\xi_m = \frac{\alpha_m}{\sigma^2\gamma_{mm}(1+\alpha_m)} = \frac{\sigma_m^2}{\sigma^4+\sigma^2\sigma_m^2\gamma_{mm}}. \tag{21}$$

For this special case, the scheme in Fig. 1 does not have the nonlinear functions and the coefficients ξ_m are defined as in (21). From (20) and (21), we see immediately that if σ_m^2 is close to zero then the mth path will not contribute to the estimation statistic.

The frequency estimate (20) is based on a linear weight addition of the path periodograms. This estimate coincides with that obtained in [2] for multipath Rayleigh-fading channels with known fading statistics. Thus, the new frequency estimator defined by (17) and (18) is a generalized ML frequency estimator for multipath Rayleigh-fading channels with known fading statistics.

B. Unknown Fading Variances

In the case of unknown fading variances, the frequency estimator knows that the fading is Rayleigh, but it does not know the path amplitude variances. This scenario is more practical than that considered in Section III-A. In order to find the ML frequency estimator under such an assumption, we have to maximize the function in (15) over the unknown parameters $\alpha_m \in [0,\infty]$, $m = 1,\ldots,M$. Such a maximization gives (see [2, App. 2])

$$\hat{\omega} = \arg\max_{\omega\in\Omega}\left\{\sum_{m=1}^{M} g(G_{\omega,m})\right\} \tag{22}$$

where

$$g(x) = g_4(x) = \ln\left[pe^{\varphi(x)} + (1-p)\right] \tag{23}$$

$$\varphi(x) = \begin{cases} 0, & \text{if } 0 \le x < 1 \\ x - \ln(x) - 1, & \text{if } x \ge 1 \end{cases} \tag{24}$$

and $p = p_0$. If $G_{\omega,m} < 1$ (or, the same, $|F_{\omega,m}|^2 < \xi_m^{-1} = \gamma_{mm}\sigma^2$) then $g_4(G_{\omega,m}) = 0$, i.e., the periodogram $|F_{\omega,m}|^2$ of the mth path does not contribute to the estimation statistic at a frequency ω. Note that the threshold $\gamma_{mm}\sigma^2$ depends on the noise variance σ^2 and does not depend on the probability p; the coefficient γ_{mm} compensates for the energy of the pilot signal in calculation of the DFT (16). The parameter p defines the contribution of the path periodogram if only it is higher than the threshold. The function $g_4(x)$ is depicted in Fig. 3 for different values of the parameter p. The smaller p the larger is the range of x where the function $g_4(x)$ is close to zero.

Thus, we have found the ML frequency estimator for multipath fading channels with a sparse impulse response when the probability p_0 of appearance of a path with a nonzero amplitude a_m at delay τ_m is known, but the variances σ_m^2 of path amplitudes (or the parameters α_m) are unknown. This ML estimator is also realized by the scheme in Fig. 1. The nonlinear function $g(x)$ is now defined in (23) and (24).

Again, we consider the special case $p_0 = 1$ which means that all paths have nonzero variances of path amplitudes, but now the variances are unknown. In this case, we get from (23) that $g_4(x) = \varphi(x)$ or $g_4(x) = g_1(x)$ [see (1)]. Thus, the particular case $p_0 = 1$ leads to the known ML frequency estimator for multipath Rayleigh-fading channels with unknown fading statistics [2], i.e., the new derived frequency estimator defined by (22)–(24) is a generalized ML frequency estimator for multipath Rayleigh-fading channels with unknown fading statistics.

IV. Simulation Results

Our implementation of the frequency estimators is based on a coarse and fine search of the peak of the combined statistic in (17) or (22); the fast Fourier transform (FFT) algorithm for the coarse search and the dichotomous algorithm for the fine search are used [6].

The computational load of the implementation includes:

1) multiplication of the received signal by the pilot signal;
2) calculation of the DFTs for all possible delays;
3) dichotomous search;
4) calculation of path periodograms;
5) nonlinear processing.

The multiplication of the complex-valued received signal by the complex-valued pilot signal requires $4MN$ real multiplications. Calculation of the DFTs by using the FFT algorithm with a zero-padding [7] requires approximately $4kMN\log_2(kN)$ multiplications and additions; the coefficient k is usually chosen within the interval $k = 2,\ldots,4$. The dichotomous search requires calculation of DM N-point DFTs where D is the number of dichotomous iterations [6]; this results in $4DMN$ real multiplications and additions. Note that D dichotomous iterations lead to improvement of the frequency resolution by 2^D times in addition to the frequency resolution of the coarse search FFT, providing an overall frequency resolution of $\delta f = (kN2^D)^{-1}$. The overall frequency resolution should be better than the expected CRLB [8]. The periodogram calculation requires $2(kMN + MD)$ real multiplications and $kMN + MD$ real additions. The nonlinear function is calculated $kMN + MD$ times; this can be done by using a lookup table. We see that for large N the computational load is mainly due to calculation of FFTs. For large N we obtain $P_{ma} \approx 4kMN\log_2(kN)$ real multiplications and additions and $P_{nl} \approx kMN$ addressing to a lookup table. For example, for $N = 255$, $M = 120$, $k = 4$, and $D = 5$, the frequency estimation requires $P_{ma} \approx 4.9 \cdot 10^6$ real multiplications and additions and $P_{nl} \approx 1.2 \cdot 10^5$ addressing to a lookup table. If the period of transmission of the pilot signal is as long as several seconds (e.g., in underwater acoustic communications [9]) this algorithm can be exploited for real-time implementation. However, in some scenarios, such a computational load may be prohibitively large. If the frequency acquision range is narrow simpler implementations based on techniques proposed in [10] can be obtained.

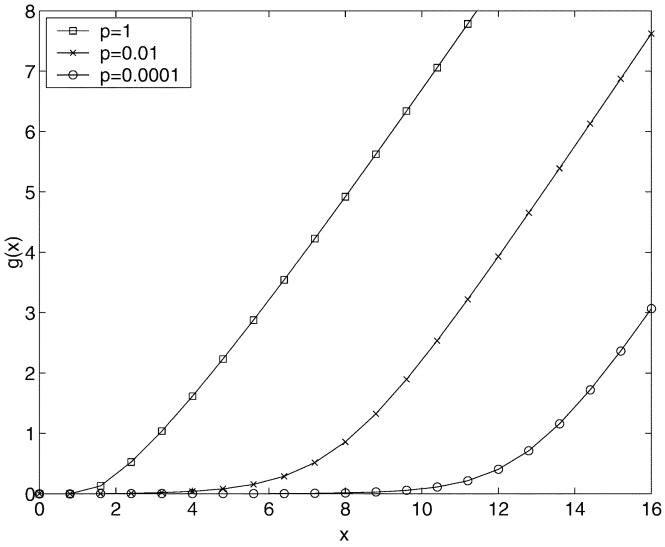

Fig. 3. Nonlinear function $g_4(x)$ for different values of the parameters p.

We compare the frequency error as a function of SNR for different nonlinear transforms $g(x)$ in the following simulation scenario. A binary maximum length sequence (m-sequence), representing a pilot signal, is transmitted through a multipath Rayleigh-fading channel with equal variances of independent path amplitudes and additive white noise. The length of the sequence is $N = 255$, the delay uncertainty is $M = 120$, and the probability of appearance of a path with a nonzero amplitude is $p_0 = 0.02$. We calculate the frequency error averaged over N_{mc} Monte Carlo simulation trials

$$\Delta f = \sqrt{\frac{1}{N_{mc}}\sum_{i=1}^{N_{mc}}(f - \hat{f}_i)^2} \tag{25}$$

where $f = \omega/2\pi$ is the true frequency and $\hat{f}_i = \hat{\omega}_i/2\pi$ is a frequency estimate in the ith simulation trial, and $N_{mc} =$

4000. In our simulation, we used $f = 0.2$; however, simulations for other frequencies within the range $f \in (-0.5, 0.5)$ have shown results close to that presented in the following. In each simulation trial, we normalize the complex envelope $A(iT)$ to produce a required SNR; a discussion on calculation of SNR in simulation trials for multipath fading channels can be found in [2].

We consider the following ML frequency estimators.

1) Estimator for deterministic multipath channels [4], which expects that all M paths have unknown nonzero deterministic amplitudes. The estimator performs a linear addition of path periodograms, and it is implemented by using $g(x) = g_2(x)$ with $p = 1$.
2) Frequency estimator for multipath Rayleigh-fading channels [2]. This estimator expects that all M paths have nonzero amplitude variances and the variances are known. The estimator performs a linear weight addition of path periodograms and the weights depend on the SNRs α_m for the received multipath signal components. This estimator is implemented by using $g(x, \alpha) = g_3(x, \alpha)$ with $p = 1$.
3) Frequency estimator for multipath Rayleigh-fading channels with unknown variances of path amplitudes [2]. This estimator expects that all M paths have nonzero amplitude variances, but the variances are unknown. This estimator is implemented by using $g(x) = g_4(x)$ with $p = 1$ [this corresponds to $g(x) = g_1(x)$].
4) Frequency estimator for deterministic multipath channels with a sparse impulse response [5]. This estimator expects that among M paths there are on average Mp_0 paths with nonzero unknown deterministic amplitudes and the parameter p_0 is known. The estimator performs a nonlinear transform of path periodograms and it is implemented by using $g(x) = g_2(x)$ with $p = p_0$.
5) Frequency estimator for multipath Rayleigh-fading channels with a sparse impulse response and known path amplitude variances. This estimator expects that among M paths there are on average Mp_0 paths with nonzero amplitude variances and the parameter p_0 and the variances are known. The estimator performs an addition of nonlinearly transformed path periodograms. The nonlinear transforms depend on the SNRs α_m of the received multipath signal components. This estimator is implemented by using $g(x, \alpha) = g_3(x, \alpha)$ with $p = p_0$.
6) Frequency estimator for multipath Rayleigh fading channels with a sparse impulse response and unknown path amplitude variances. This estimator expects that among all M paths there are on average Mp_0 paths with nonzero amplitude variances, the parameter p_0 is known, but the variances are unknown. The estimator sums nonlinearly transformed path periodograms; it is implemented by using $g(x) = g_4(x)$ with $p = p_0$.

Figs. 4–6 show the dependence of the frequency error (25) on SNR for the three nonlinear functions $g_2(x)$, $g_3(x)$, and $g_4(x)$, respectively. For each function, we consider the following values of the parameter p:

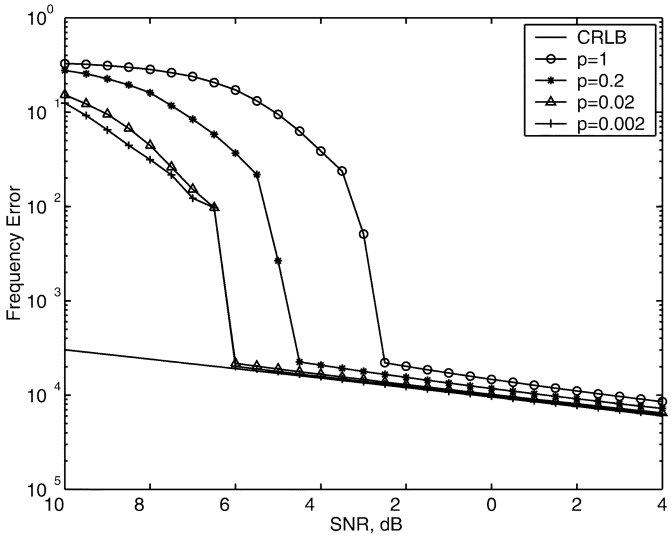

Fig. 4. Nonlinear function $g_2(x)$. Dependency of the frequency error on SNR; $N = 255$, $M = 120$, and $p_0 = 0.02$.

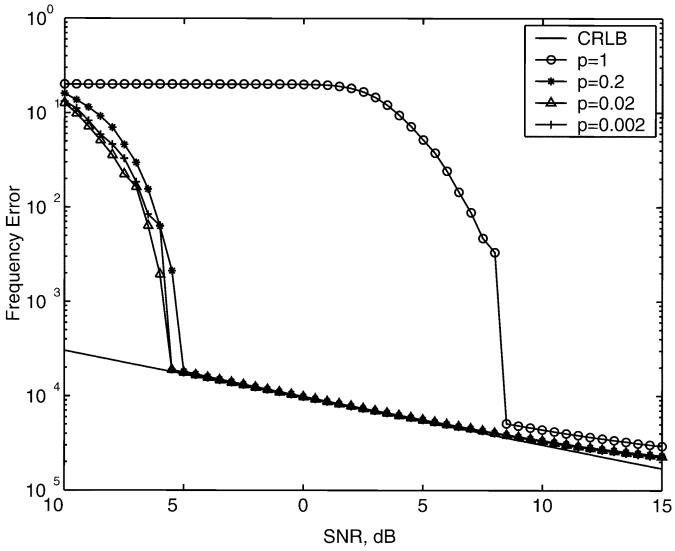

Fig. 5. Nonlinear function $g_3(x, \alpha)$. Dependency of the frequency error on SNR; $N = 255$, $M = 120$, and $p_0 = 0.02$.

1) $p = 1$ corresponding to ML frequency estimation in a multipath channel with unknown path amplitudes which are either deterministic (Fig. 4) or Gaussian random variables with known variances (Fig. 5) or Gaussian random variables with unknown variances (Fig. 6);
2) $p = 0.2 > p_0$;
3) $p = p_0 = 0.02$ corresponding to the theoretical optimal value of p;
4) $p = 0.002 < p_0$.

Figs. 4–6 also show the CRLB for the frequency error in a single path channel [7]:

$$\sigma_{\mathrm{CRLB}} = \sqrt{\frac{3}{(2\pi^2 N(N^2-1)\mathrm{SNR})}}. \tag{26}$$

We can conclude the following.

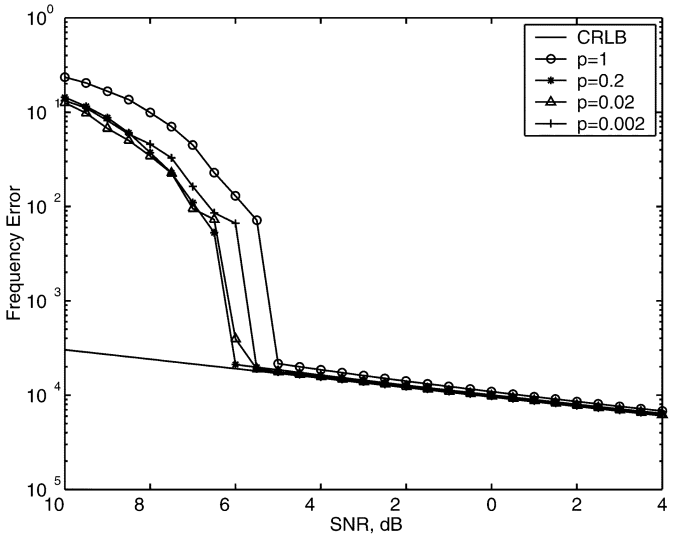

Fig. 6. Nonlinear function $g_4(x)$. Dependency of the frequency error on SNR; $N = 255$, $M = 120$, and $p_0 = 0.02$.

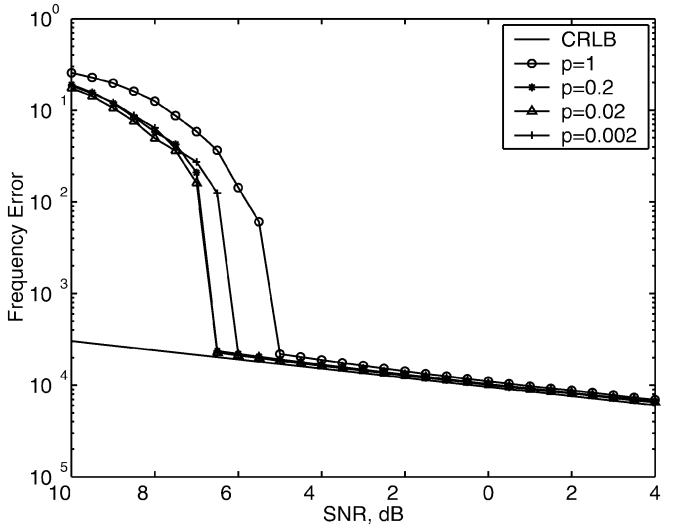

Fig. 7. Nonlinear function $g_4(x)$. Dependency of the frequency error on SNR; $N = 255$, $M = 120$, and $L = 2$.

1) All the nonlinear functions provide very close minimal SNR thresholds (between -5.5 and -6 dB) and the minimum is achieved at approximately $p = p_0$.
2) The functions $g_3(x)$ and $g_4(x)$ with the parameter $p = p_0$ provide about the same minimal SNR threshold in spite of the fact that the frequency estimator with the function $g_3(x)$ uses more *a priori* information about the channel (knowledge of the path amplitude variances) than the estimator with the function $g_4(x)$. Thus, the use of the frequency estimator with the function $g_4(x)$ is preferable because it requires less knowledge of the channel, while providing approximately the same accuracy performance.
3) The estimators with the functions $g_3(x)$ and $g_4(x)$ demonstrate a weak sensitivity to knowledge of the parameter p_0. The SNR threshold varies within approximately 0.5 dB when the parameter p varies within two orders: $0.2 < p < 0.002$. It means that there is no necessity to know very precisely the expected number of nonzero paths; this feature is useful for practical applications.
4) The frequency estimator optimized for multipath Rayleigh-fading channels with known nonzero path amplitude variances (i.e., when $g(x) = g_3(x, \alpha)$ and $p = 1$) demonstrates a poor accuracy performance. This is because the estimator expects that all $M = 120$ delays contain paths with nonzero amplitude variances which are equal to each other, while, in reality, the number of such paths is on average only $E\{L\} = 120 \cdot 0.02 = 2.4$.
5) The frequency estimator optimized for deterministic multipath channels with unknown nonzero path amplitudes (i.e., when $g(x) = g_2(x)$ and $p = 1$) also demonstrates a relatively poor accuracy performance; the SNR threshold $(-2.5$ dB$)$ is about 3.5 dB higher than the minimum. However, it is about 11 dB less than that of the estimator for multipath Rayleigh fading channels with known nonzero path amplitude variances.
6) At SNRs higher than the SNR threshold, all the estimators demonstrate accuracy performance close to the CRLB. However, at SNRs higher than about 10 dB the frequency error departs from the CRLB; this behavior is due to nonzero autocorrelations of the pilot signal. This effect is well seen in Fig. 5. Note that the pilot signal used in the simulation possesses an autocorrelation with side lobes as large as 7% of the main lobe.

We now consider a multipath channel with a fixed number of multipath components L and arbitrary continues delays t_l within a delay uncertainty interval $[0, (M-1)T]$. In each simulation trial, we choose random delays from a uniform distribution on $[0, (M-1)T]$. We also model the transmit and receive filters with the root-raised cosine impulse response and a rolloff factor of 0.22 [11]. This allows us to consider more realistic scenarios described by (11) and (12). Figs. 7 and 8 show the dependence of the frequency error on SNR for the nonlinear function $g_4(x)$ with $L = 2$ and $L = 3$; note that simulation results in Fig. 6 correspond to the average number of multipath components $E\{L\} = 2.4$ which is between $L = 2$ and $L = 3$. It can be seen that the increase in the number of multipath components from $L = 2$ (Fig. 7) to $L = 3$ (Fig. 8) increases the threshold SNR by only 1 dB or less. We also see that results in Figs. 7 and 8 are very close to that in Fig. 6. Thus, despite that the channel model used for derivation of the ML frequency estimator was based on the assumptions of uncorrelated path amplitudes and path delays being multiples of the sampling period, the simulation results in Figs. 7 and 8 show that this estimator demonstrates approximately the same performance in a more realistic channel with correlated path amplitudes and fractional path delays. Fig. 9 shows the dependence of the frequency error on the estimated frequency $f = \omega/(2\pi)$ for SNR $= 0$ dB. It can be seen that, in a wide frequency range, the accuracy is close to the CRLB in a single-path channel.

Thus, the use of *a priori* information about the mean number of paths in the channel allows a significant improvement of the accuracy performance relative to the case of $p = 1$. At high SNRs, the variance of the frequency error is close to the CRLB. The performance deterioration is not significant for nonoptimal

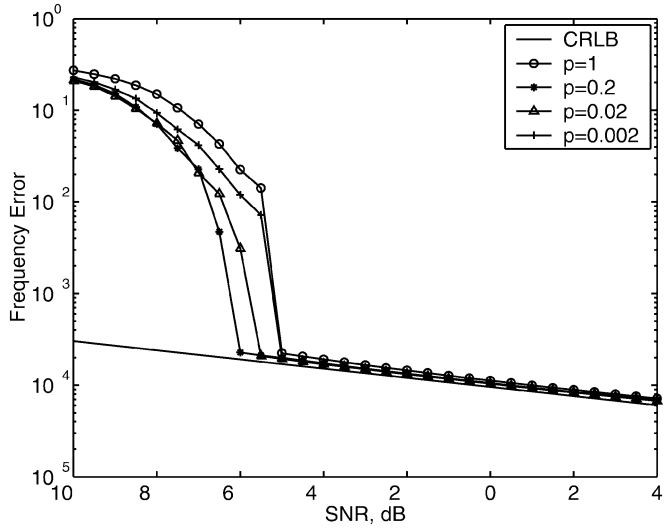

Fig. 8. Nonlinear function $g_4(x)$. Dependency of the frequency error on SNR; $N = 255$, $M = 120$, and $L = 3$.

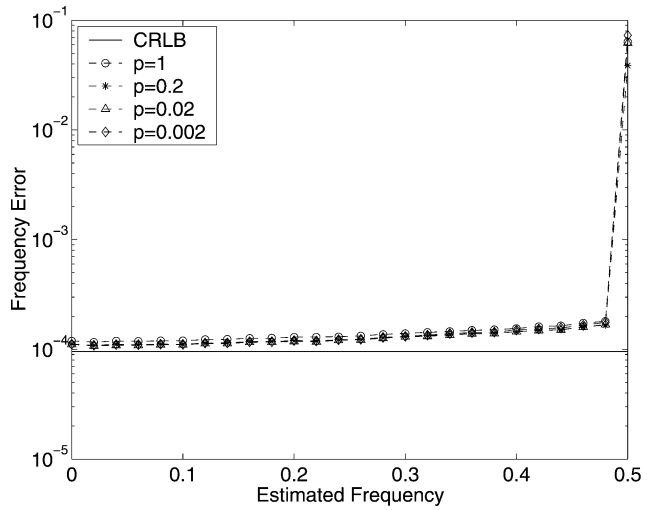

Fig. 9. Nonlinear function $g_4(x)$. Dependency of the frequency error on the estimated frequency; $N = 255$, $M = 120$, and $L = 3$.

choice of the parameter p, which shows that the algorithm performance is not very sensitive to this information.

V. Conclusion

We have obtained new ML frequency estimation algorithms for multipath Rayleigh-fading channels with a sparse impulse response when a probability of appearance of a path with a nonzero amplitude at each possible delay within a timing uncertainty interval is known, and the variances of path amplitudes are either known or unknown. These estimators are based on nonlinear transforms of path periodograms and the nonlinear functions are different for the cases of known and unknown fading statistics. Nonlinear functions allow the frequency estimators to accumulate the periodograms of strong paths rejecting weak paths. Frequency estimators with nonlinear transforms of path periodograms were recently obtained for both multipath channels possessing a sparse impulse response with unknown deterministic path amplitudes [5] and multipath Rayleigh-fading channels with unknown path amplitude variances [2]. Here, we show that the new nonlinear transforms obtained give us generalized frequency estimation algorithms for multipath fading channels, depending on the parameter p_0, the probability of appearance of nonzero path amplitudes. In particular, for $p_0 = 1$ they lead to known frequency estimators for multipath Rayleigh-fading channels with either known or unknown nonzero path amplitude variances.

The simulations have shown that all nonlinear functions provide very close SNR thresholds, which are significantly lower than that of estimators not accounting for the channel sparseness. Our estimators also demonstrate a better accuracy performance at high SNRs for a large timing uncertainty; the frequency error approaches the CRLB for a one-path AWGN channel. The accuracy performance of the estimators is not very sensitive to knowledge of the channel sparseness; the uncertainty in the average number of paths may be as large as a factor of 10. The use of the nonlinear function $g_4(x)$ is preferable because it requires less knowledge of the channel, while providing approximately the same accuracy performance as the other estimators at optimal parameters, and the difference of SNR thresholds for this function is minimal.

Appendix
PDF $\mathbf{p}(\mathbf{z}|\omega)$

In order to derive the ML frequency estimation algorithm, we use the Bayesian approach by integrating out the nuisance parameters a_m and χ_m, $m = 1, \ldots, M$. We can write

$$\mathbf{p}(\mathbf{z}|\omega, \mathbf{x}) = \int_{-\infty}^{\infty} \mathbf{p}(\mathbf{z}|\omega, \mathbf{x}, \mathbf{a}) \mathbf{f}_{\mathbf{a}}(\mathbf{a}) d\mathrm{Re}[\mathbf{a}] d\mathrm{Im}[\mathbf{a}] \quad (27)$$

where Re[·] and Im[·] denote, respectively, the real and imaginary parts of a complex-valued number. The pdf $\mathbf{p}(\mathbf{z}|\omega, \mathbf{x}, \mathbf{a})$ is defined by (7), the pdf $\mathbf{f}_{\mathbf{a}}(\mathbf{a})$ is defined by (8). Then, we can write

$$\mathbf{p}(\mathbf{z}|\omega) = \int_{-\infty}^{\infty} \mathbf{p}(\mathbf{z}|\omega, \mathbf{x}) \mathbf{f}_{\mathbf{x}}(\mathbf{x}) d\mathbf{x} \quad (28)$$

where the pdf $\mathbf{f}_{\mathbf{x}}(\mathbf{x})$ is defined in (10).

We start our derivation for arbitrary noise and fading covariance matrices $\mathbf{R}_{\mathbf{n}}$ and $\mathbf{R}_{\mathbf{a}}$. Then, we will apply our assumption that the matrices are diagonal to show at what stage they are important for the derivation. Here, we will use notations from [2]. Substituting (7) and (8) in (27) yields

$$\mathbf{p}(\mathbf{z}|\omega, \mathbf{x}) = c_0 \int \exp\left\{2Re\left[\mathbf{a}^H \mathbf{L}_\omega\right] - \mathbf{a}^H \mathbf{\Gamma}_\omega \mathbf{a}\right\} \times \mathbf{f}_{\mathbf{a}}(\mathbf{a}) d\mathrm{Re}[\mathbf{a}] d\mathrm{Im}[\mathbf{a}] \quad (29)$$

where

$$\mathbf{L}_\omega = \mathbf{X}\mathbf{\Phi}^H \mathbf{\Lambda}_\omega^H \mathbf{R}_{\mathbf{n}}^{-1} \mathbf{z} \quad (30)$$

$$\mathbf{\Gamma}_\omega = \mathbf{X}\mathbf{\Phi}^H \mathbf{\Lambda}_\omega^H \mathbf{R}_{\mathbf{n}}^{-1} \mathbf{\Lambda}_\omega \mathbf{\Phi} \mathbf{X} \quad (31)$$

and $c_0 = \pi^{-N}|\mathbf{R_n}|^{-1}\exp\left\{-\mathbf{z}^H\mathbf{R_n^{-1}}\mathbf{z}\right\}$. Integrating in (29) results in (e.g., see [2, App. 1])

$$\mathbf{p}(\mathbf{z}|\omega,\mathbf{x}) = \frac{c_0 e^{W_\omega}}{|\mathbf{R_a}\boldsymbol{\Gamma}_\omega + \mathbf{I}|} \tag{32}$$

where

$$W_\omega = \mathbf{L}_\omega^H\left(\boldsymbol{\Gamma}_\omega + \mathbf{R_a^{-1}}\right)^{-1}\mathbf{L}_\omega. \tag{33}$$

We now assume that the noise covariance matrix is diagonal: $\mathbf{R_n} = \sigma^2\mathbf{I}_N$, where $\mathbf{I}_N$ is an $N \times N$ identity matrix, i.e., the noise samples are uncorrelated and have equal variances σ^2. Then, from (30) and (31), using the identity $\boldsymbol{\Lambda}_\omega^H\boldsymbol{\Lambda}_\omega \equiv \mathbf{I}_N$, we obtain $\mathbf{L}_\omega = \sigma^{-2}\mathbf{X}\mathbf{F}_\omega$ and $\boldsymbol{\Gamma}_\omega = \mathbf{X}\boldsymbol{\Gamma}\mathbf{X}$, where elements $F_{\omega,m}$ of the vector $\mathbf{F}_\omega$ are the DFTs

$$F_{\omega,m} = \sum_{i=0}^{N-1} z(iT)s^*(iT-\tau_m)e^{-j\omega iT} \tag{34}$$

and $\boldsymbol{\Gamma} = \sigma^{-2}\boldsymbol{\Phi}^H\boldsymbol{\Phi}$ is the correlation matrix of the transmitted signal normalized by the noise variance.

We consider now the case of independent fluctuations of path amplitudes, when the covariance matrix $\mathbf{R_a}$ is diagonal: $\mathbf{R_a} = \text{diag}\left(\sigma_1^2,\ldots,\sigma_M^2\right)$. Let also $\boldsymbol{\Gamma}$ be approximated by a diagonal matrix $\boldsymbol{\Gamma} = \sigma^{-2}\text{diag}(\gamma_{11},\gamma_{22},\ldots,\gamma_{MM})$ where $\gamma_{mn} = [\boldsymbol{\Phi}^H\boldsymbol{\Phi}]_{mn} = \sum_{i=0}^{N-1} s^*(iT-\tau_m)s(iT-\tau_n)$. These assumptions result in the following simplification.

1) The matrix $\boldsymbol{\Gamma}_\omega$ is diagonal with the diagonal elements $\sigma^{-2}\chi_m\gamma_{mm}$, $m = 1,\ldots,M$.
2) The matrix $\mathbf{B} = \boldsymbol{\Gamma}_\omega + \mathbf{R_a^{-1}}$ is diagonal with the diagonal elements $b_{mm} = \sigma^{-2}\chi_m\gamma_{mm} + \sigma_m^{-2}$, $m = 1,\ldots,M$.
3) The matrix $\mathbf{B_x} = \mathbf{X}^H\mathbf{B}^{-1}\mathbf{X}$ is diagonal with the diagonal elements $\chi_m b_{mm}^{-1}$, $m = 1,\ldots,M$.
4) The matrix $\mathbf{C} = \mathbf{R_a}\boldsymbol{\Gamma}_\omega + \mathbf{I}$ is diagonal with the diagonal elements $\sigma^{-2}\chi_m\gamma_{mm}\sigma_m^2 + 1$, $m = 1,\ldots,M$.
5) From (33) we have

$$\begin{aligned} W_\omega &= \sigma^{-4}\mathbf{F}_\omega^H\mathbf{B_x}\mathbf{F}_\omega \\ &= \sigma^{-4}\sum_{m=1}^{M}\chi_m b_{mm}^{-1}|F_{\omega,m}|^2. \end{aligned} \tag{35}$$

Now, we can rewrite $\mathbf{p}(\mathbf{z}|\omega,\mathbf{x})$ in (32) as

$$\begin{aligned} \mathbf{p}(\mathbf{z}|\omega,\mathbf{x}) &= c_0\frac{\exp\left(\sigma^{-4}\mathbf{F}_\omega^H\mathbf{B_x}\mathbf{F}_\omega\right)}{|\mathbf{C}|} \\ &= c_0\prod_{m=1}^{M} J_m(\omega,\chi_m) \end{aligned} \tag{36}$$

where

$$J_m(\omega,\chi_m) = \frac{\exp\left(\sigma^{-4}\chi_m b_{mm}^{-1}|F_{\omega,m}|^2\right)}{\sigma^{-2}\chi_m\gamma_{mm}\sigma_m^2 + 1}. \tag{37}$$

The factor $J_m(\omega,\chi_m)$ depends on the random binary parameter χ_m taking on a value of either $\chi_m = 1$ or $\chi_m = 0$. If $\chi_m = 0$, then from (37), we obtain $J_m(\omega,\chi_m) = 1$. If $\chi_m = 1$, we obtain

$$J_m(\omega,\chi_m) = \frac{1}{\sigma^{-2}\gamma_{mm}\sigma_m^2 + 1}\exp\left(\frac{|F_{\omega,m}|^2}{\sigma^2\gamma_{mm} + \sigma^4\sigma_m^{-2}}\right). \tag{38}$$

Denoting $\alpha_m = \sigma_m^2\gamma_{mm}/\sigma^2$, this value can be interpreted as an SNR of mth received multipath component. Then, (38) becomes

$$J_m(\omega,\chi_m) = \frac{1}{1+\alpha_m}\exp\left\{\frac{G_{\omega,m}\alpha_m}{1+\alpha_m}\right\} \tag{39}$$

where $G_{\omega,m} = \xi_m|F_{\omega,m}|^2$ and $\xi_m = (\sigma^2\gamma_{mm})^{-1}$.

In order to find $\mathbf{p}(\mathbf{z}|\omega)$, we integrate out the nuisance parameters χ_m in $\mathbf{p}(\mathbf{z}|\omega,\mathbf{x})$. Accounting for (10), (36), and (39) from (28), we finally obtain

$$\begin{aligned} \mathbf{p}(\mathbf{z}|\omega) &= c_0\int_{-\infty}^{\infty}\prod_{m=1}^{M} J(\omega,\chi_m) \\ &\quad\times\left[p_0\delta(\chi_m-1) + (1-p_0)\delta(\chi_m)\right]d\chi_m \\ &= c_0\prod_{m=1}^{M}\left[\frac{p_0}{1+\alpha_m}\exp\left(\frac{G_{\omega,m}\alpha_m}{1+\alpha_m}\right)\right. \\ &\quad\left.+(1-p_0)\right]. \end{aligned} \tag{40}$$

REFERENCES

[1] H. Meyr, M. Moeneclaey, and S. Fechtel, *Digital Communication Receivers, Synchronization, Channel Estimation, and Signal Processing*. New York: Wiley, 1998.

[2] V. M. Baronkin, Y. V. Zakharov, and T. C. Tozer, "Frequency estimation in slowly fading multipath channels," *IEEE Trans. Commun.*, vol. 50, pp. 1848–1859, Nov. 2002.

[3] M. Morelli and U. Mengali, "Carrier-frequency estimation for transmission over selective channels," *IEEE Trans. Commun.*, vol. 48, pp. 1580–1589, Sept. 2000.

[4] V. M. Baronkin, Y. V. Zakharov, and T. C. Tozer, "Maximum likelihood single tone frequency estimation in multipath channels," *IEE Proc. Commun.*, vol. 148, no. 6, pp. 400–404, Dec. 2001.

[5] ——, "Frequency estimator for multipath channels with sparse impulse response," *Electron. Lett.*, vol. 37, pp. 85–86, Jan. 2001.

[6] Y. V. Zakharov and T. C. Tozer, "Frequency estimator with dichotomous search of periodogram peak," *Electron. Lett.*, vol. 35, pp. 1608–1609, Sept. 1999.

[7] D. C. Rife and R. R. Boorstyn, "Single-tone parameter estimation from discrete-time observations," *IEEE Trans. Inform. Theory*, vol. IT-20, pp. 591–598, Sept. 1974.

[8] F. Gini and G. B. Giannakis, "Frequency offset and symbol timing recovery in flat-fading channels: A cyclostationary approach," *IEEE Trans. Commun.*, vol. 46, pp. 400–411, Mar. 1998.

[9] Y. V. Zakharov and V. P. Kodanev, "Experimental study of an underwater acoustic communication system with pseudonoise signals," *Acoust. Phys.*, vol. 40, no. 5, pp. 799–808, 1994.

[10] Y. V. Zakharov, V. M. Baronkin, and T. C. Tozer, "DFT-based frequency estimators with narrow acquisition range," *Inst. Elect. Eng. Proc. Commun.*, vol. 148, no. 1, pp. 1–7, Feb. 2001.

[11] "The ETSI UMTS terristrial radio access (UTRA) ITU-R RTT candidate submission," ETSI, 1998.

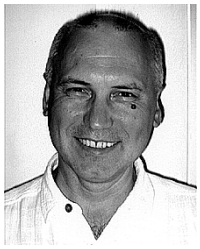

Yuriy V. Zakharov (M'01) received the M.Sc. and Ph.D. degrees in electrical engineering from the Moscow Power Engineering Institute, Moscow, Russia, in 1977 and 1983, respectively.

From 1977 to 1983, he was an Engineer with the Special Design Agency, Moscow Power Engineering Institute. From 1983 to 1999, he was a Head of Laboratory, the N. N. Andreev Acoustics Institute, Moscow. From 1994 to 1999, he worked for Nortel, Moscow, as a DSP Group Leader. Since 1999, he has been with the University of York, York, U.K., as a Senior Research Fellow. His interests include signal processing and communications, including underwater acoustic systems, mobile communications, multimedia algorithms for telephone networks, and speech processing.

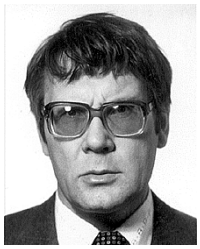

Vladimir M. Baronkin received the M.Sc. and Ph.D. degrees in electrical engineering from the Moscow University of Communications, Moscow, Russia, in 1961 and 1973, respectively.

From 1963 to 1976, he was a Researcher with the Radiotechnical Systems Laboratory, Moscow. Since 1976, he has been the Head of the Signal Processing Laboratory, the N. N. Andreev Acoustics Institute, Moscow. He is also an Associate Professor with the State Engineering Physics Institute, Moscow, and the University of Radio Engineering, Electronics and Automatic, Moscow. He has published over 70 joumal and conference papers. His research interests include statistical signal processing, with specific attention to adaptive space-time signal processing, speech processing, estimation, and testing hypothesis theory.

Dr. Baronkin is a member of the Russian Acoustical Society.

Tim C. Tozer (M'81) received the degree in engineering from the University of Cambridge, Cambridge, U.K., in 1969.

After a few years as a Microwave Systems Engineer with Philips Research Laboratories, Redhill, U.K., he joined the University of Kent, Canterbury, U.K., where he developed an interest in spread-spectrum techniques. In 1979, he moved to the Royal Signals and Radar Establishment, Malvern, U.K., where he developed military satellite communications. He has worked closely with industry and has served on several international committees. Since 1987, he has been Head of the Communications Research Group, University of York, York, U.K. He is active internationally in presenting short courses and workshops on satellite communications and on communications from high altitude platforms. He is also a Director of SkyLARC Technologies Ltd., York, U.K., a company developing wireless broadband solutions with emphasis on HAPs. He is responsible for numerous research contracts from industry and other agencies and is the named author of over 100 publications. His current interests include wireless communications systems and small-dish satellite communications (VSATs).